Journal of Materials Chemistry B

ROYAL SOCIETY OF CHEMISTRY

PAPER

View Article Online
View Journal | View Issue

Cite this: J. Mater. Chem. B, 2024, 12, 2807

Injectable polyoxazoline grafted hyaluronic acid thermoresponsive hydrogels for biomedical applications†

Morgane Morel,[ab] Mathieu Madau,[a] Didier Le Cerf,[a] Virginie Dulong,[a] Anne-Claire Groo,[b] Aurélie Malzert-Fréon[b] and Luc Picton *[a]

Received 10th September 2023,
Accepted 14th February 2024

DOI: 10.1039/d3tb02108d

rsc.li/materials-b

Injectable thermosensitive hydrogels based on hyaluronic acid (HA) grafted with lower critical solution temperature (LCST) polyoxazoline (copolymers of poly(isopropyl-*co*-butyl oxazoline)) or P(iPrOx-*co*-BuOx) have been elaborated with tunable solution/gel temperature transitions and gel state elastic modulus. A suitable HA-*g*-P(iPrOx-*co*-BuOx-67/33)-0.10 sample with an iPrOx/BuOx ratio of 67/33, a polymerization degree (DP) of 25, a substitution degree (DS) of 10%, and displaying thermally induced gelling character with elastic (G') and viscous (G'') moduli crossover points at 25 °C and a G' at 37 °C around 80 Pa has been chosen for medical application. Hydrogels obtained with HA-*g*-P(iPrOx-*co*-BuOx-67/33)-0.10 exhibited high stability at 37 °C and excellent injectability properties with full and quick reversibility. The incorporation of a secondary network (HA), until 35 wt%, into the thermosensitive hydrogel also demonstrated very good stability and injectability.

1. Introduction

Hydrogels are tridimensional crosslinked networks soluble in water made from artificial or natural polymers. They can be created under several shapes such as coatings and films, micro and nanoparticles, *etc.*[1–3] Hydrogels are present in a lot of applications, especially in tissue engineering,[4] regenerative medicine,[5] diagnostics,[6] cell immobilization,[7] and controlled delivery of active agents.[8] Hydrogels can be classified into chemical or physical hydrogels, with chemical hydrogels being made of covalent crosslinking,[9] while physical hydrogels[10] are instead made of non-covalent bonds (ionic interaction, van der Waals interactions, hydrogen bonds, *etc.*). Physical hydrogels are preferred for injection treatments because of their reversibility, and in some cases, they can respond to external stimuli such as temperature, pH, electric field, *etc.*

The number of studies on injectable hydrogels has been growing steadily in the biomedical field for many years. This is because injectable hydrogels offer several advantages over conventional methods of administration (intravenous, intranasal, and oral). In fact, injectable hydrogels enable the therapy to be delivered directly to the target site, thus avoiding problems of diffusion into "healthy" areas of the human body. This method also overcomes certain barriers (such as the blood–brain barrier) which limit access to certain molecules, so that the dose of delivered therapy is better controlled.[11–14]

For *in situ* injection, thermosensitive physical hydrogels that undergo a transition from the liquid state at room temperature to the gel state once they arrive at the desired site with the help of body temperature are very interesting materials as they make the injection process easier.[8,15–17] They can be obtained by grafting LCST (lower critical solution temperature) polymers onto a water-soluble polymer. LCST polymers are water soluble below the LCST temperature and precipitate above the LCST temperature. This phenomenon is explained by the fact that heat causes the polymer/polymer interactions to be favorable over the polymer/solvent interactions. As a matter of fact, thermosensitive polymers lead to physical crosslinking nodes between the LCST polymer chains at a given temperature making it possible to form a gel.[10,18–20]

At present, there are several types of LCST polymers known, such as some polyether amines (Jeffamine®), PNIPAM, or some types of polyoxazolines (POXs).[18,21–25] However, we'll be focusing solely on polyoxazolines because, unlike Jeffamine® or PNIPAM, POXs appear more biocompatible, allow easier control of the gelation temperature, and, even more strikingly, an almost spontaneous resulting sol–gel transition.[20,26–29]

During this work, we chose to create an injectable thermoresponsive hydrogel thanks to hyaluronic acid (HA). Hyaluronic acid is an anionic polysaccharide that is completely

[a] Univ Rouen Normandie, CNRS, PBS UMR6270, F-76000 Rouen, France. E-mail: luc.picton@univ-rouen.fr
[b] Univ Caen Normandie, CERMN, UR4258, F-14000 Caen, France

† Electronic supplementary information (ESI) available. See DOI: https://doi.org/10.1039/d3tb02108d

biocompatible and biodegradable due to its ubiquity in the human body especially in the extracellular matrix but also in various conjunctive tissues.[18,30–33] Unfortunately, hyaluronic acid doesn't naturally form a heat-sensitive hydrogel, so we decided to graft polyoxazoline (POX) copolymers displaying an LCST behavior on it. This work follows our previous study focusing on the sol–gel transition of HA grafted with suitable POX copolymers (*i.e.*, poly(isopropyl-*co*-butyl-oxazoline) or P(iPrOx-*co*-BuOx)).[34] The thermal transition can then be perfectly controlled by adjusting the IPrOx/BuOx ratio, the degree of polymerization (DP), and the degree of substitution (DS) of the LCST polymer.[34,35]

Indeed, the present work exploits this synthesis route to design an easily and controlled injectable thermo-sensitive hydrogel that is stable at 37 °C with suitable, quick, and reversible gelation. In contrast to our previous study,[34] we have here set the synthesis conditions to obtain these injectable heat-sensitive hydrogels compatible with biomedical use. However, in this study, no specific application or specific site of injection was sought; hence, the following study focuses on the simulated injectability of a thermosensitive and biocompatible system in the body at 37 °C.

The injectability of the hydrogel will be thoroughly evaluated. Moreover, the robustness of the hydrogel properties when inserting a secondary HA network will be assessed. The secondary HA network could then be grafted with drug molecules to devise a hydrogel-based drug delivery system.

2. Experimental

2.1 Materials

Hyaluronic acid sodium salt (Na–HA) from streptococcus equi bacterial glycosaminoglycan polysaccharide (1.2 MDa), tetrabutylammonium hydroxide (TBAOH), 2-*n*-isopropyl-2-oxazoline (iPrOx), 2-*n*-butyl-2-oxazoline (BuOx), methyl-*p*-toluenesulfonate, chloroform-D ($CDCl_3$), sodium deuteroxide (NaOD), deuterium oxide (D_2O), boric acid, (4-(dimethylamino)benzaldehyde) (DMAB), acetic acid 96%, hyaluronidase from bovine testes type IV-S and anhydrous acetonitrile were purchased from Sigma-Aldrich. Dimethylsulfoxide anhydrous (DMSO), sodium chloride (NaCl), sodium hydroxide pellets (NaOH), and acetone were purchased from VWR. Potassium hydroxide (KOH) and hydrochloric acid 35% were purchased from Prolabo. Potassium hydrogen phthalate was purchased from Fisher Chemicals and potassium nitrate from Wako. The phosphate buffer (0.1 M; pH 7.4) was made from sodium dihydrogen phosphate monohydrate from AppliChem and di-sodium hydrogen phosphate dihydrate from Merck-Millipore. Milli-Q water used was purified using the Milli-Q water reagent system from Millipore (MA, USA).

2.2 Synthesis of HA-PiPrOx-*co*-PBuOx

HA-*g*-P(iPrOx-*co*-BuOx) was synthesized as shown previously.[34] Briefly, Na–HA was converted into tetrabutylammonium hyaluronate (TBA-HA) in order to be soluble in a polar aprotic solvent (DMSO). The polymerization of 2-*n*-isopropyl-2-oxazoline (iPrOx) and 2-*n*-butyl-2-oxazoline (BuOx) (at a theoretical molar ratio of 68/32, and a theoretical polymerization degree (DP) of 30) has been done through living cationic ring-opening polymerization (CROP) at 70 °C during 24 h, using methyl-*p*-toluenesulfonate as the initiator. After that, the termination step was realized with the use of TBA-HA (dissolved in DMSO) as a termination agent for 24 h at 60 °C.[35] Dialysis (with Spectra/Por®4 dialysis membrane MWCO: 12–14 kDa from Repligen), lyophilization, and acetone washing were performed to purify the product. ^{1}H NMR (in D_2O and NaOD) and rheological (in NaCl 0.9% (0.15 M)) measurements have been successful in confirming the efficiency of the grafting.

2.3 Characterization methods

2.3.1 ^{1}H NMR. The HA-*g*-P(iPrOx-*co*-BuOx) samples were characterized by ^{1}H NMR spectroscopies (300 MHz from Bruker). Samples were prepared and analyzed as shown in the previous article.[34] Briefly, the P(iPrOx-*co*-BuOx) polymer was dissolved in deuterated chloroform, and HA-*g*-P(iPrOx-*co*-BuOx) samples were prepared in D_2O/NaOD (NaOD 0.125 M) at a concentration of 5 g L^{-1}. P(iPrOx-*co*-BuOx) was characterized to determine the polymerization degree of the copolymer but also to confirm the complete polymerization before the termination step. HA-*g*-P(iPrOx-*co*-BuOx) samples were characterized to evaluate the efficiency of grafting by determining the substitution degree (DS) after purification.

2.3.2 Rheology. Rheological measurements were performed using a Discovery H-2 hybrid-controlled stress rheometer from the TA instrument (Waters, UK) in order to monitor different behaviors. Most of the studied solutions were based on HA-*g*-P(iPrOx-*co*-BuOx-67/33)-0.10 prepared at 15 g L^{-1} in 0.9% NaCl (cold magnetic stirring for 48 h). Double wall concentric cylinder geometry (dimensions: inside cup diameter: 30.21 mm; inside bob diameter: 32 mm; outside bob diameter: 35.02 mm; outside cup diameter: 37.02 mm; inner cylinder height: 54.98 mm and immersed height: 54.48 mm from TA Instrument) was used for all measurements. Dynamic measurements were conducted in the linearity domain of viscoelastic properties. Temperature ramps (Peltier temperature control) in the dynamic mode (at 1 Hz) were then carried out from 10 to 60 °C at a heating rate of 0.5 °C min^{-1} (0.1 Pa and 1 Hz). A round trip was performed to prove the reversibility of the system.

Hydrogel stability was then monitored by tracking elastic (G') and viscous (G'') moduli over time at 37 °C for 24 hours (0.1 Pa and 1 Hz).

For injectability measurements, the samples were subjected to various stresses ranging from 5 to 100 Pa for 5 min at 20 °C or injected in the geometry using different types of syringes and needles. They were then placed under a stress of 0.1 Pa for 5 min at 20 °C. Finally, the temperature was raised to 37 °C (0.1 Pa) for 10 min.

Flow measurements have been carried out with up (10′) and down (10′) applied shear rates scans between 0.1 to 1000 s^{-1}.

2.3.3 Total organic carbon (TOC) measurements. TOC measurements were carried out using a Shimadzu total organic carbon analyzer (Japan). Calibration curves were made with potassium hydrogenophthalate (HPP) at 500 ppm. The purpose of these analyses was to monitor the possible dissolution of the hydrogel in an excess of solvent (in this case NaCl 0.1 5 M) at 37 °C. To this end, an experiment was set up at 37 °C, in which the hydrogel was gelled in a flask, and excess solvent (10 mL) was placed on top (supernatant). Samples (7 mL of supernatant) were then taken at different times and replaced with fresh supernatant. Then, these samples are diluted twice and analyzed using the total organic carbon analyzer. The objective was to determine the carbon content of the supernatant over time, and thus return to the potentially released polymer concentration in the supernatant.

2.3.4 Swelling measurement and stability. Swelling measurements have been done to confirm the results obtained by TOC and rheology on hydrogel stability with or without excess solvent. To summarize, the dry hydrogel was weighed and then dissolved (at 4 °C) with NaCl 0.15 M to achieve a concentration of 15 g L^{-1}. Once in solution, it was gelled at 37 °C and weighed again. Once the hydrogel was obtained in its gelled form, excess solvent was added to its surface. At different times, the excess solvent was removed, and the mass of the hydrogel was remeasured. This analysis was repeated throughout the study. The swelling ratio (Q) was calculated according to eqn (1):

$$Q = \frac{\text{hydrated hydrogel} - \text{dry hydrogel}}{\text{dry hydrogel}} \quad (1)$$

2.3.5 Enzymatic degradation (Reissig method). To evaluate the stability of the hydrogel in the human body, a preliminary enzymatic degradation study was carried out using hyaluronidase (HAase). Indeed, hyaluronidase is the enzyme that naturally hydrolyzes glycosaminoglycan (hyaluronic acid), so it is found in large amounts in the human body. Its activity depends not only on its location in the body but also on whether the surrounding tissue is healthy or infected/inflamed.[36] For example, in many tumors, hyaluronidase is overexpressed in the tumor microenvironment.[37] To study the hydrogel's enzymatic degradation, we used the Reissig method (1955).[38] To sum up, this method quantifies the amount of reducing sugar (*N*-acetylglucosamine) resulting from the cutting of β(1–4) glycosidic bonds *via* a colorimetric titration method. To quantify the reducing ends groups of the hydrogel, a calibration curve for the method was first prepared, ranging from 0.0045 to 2 mmol L^{-1} of *N*-acetylglucosamine in NaCl 0.15 M. For the hydrogel, a 15 g L^{-1} solution in NaCl 0.15 M was prepared and 10 mL of this solution was placed at 37 °C while 10 mL were placed at room temperature. This experiment allowed the comparison of the appearance of the reducing end groups when the hydrogel was in liquid or in gel form in the presence of HAase (100 μL at 1 mg mL^{-1}). Various samples were taken throughout the study, and 200 μL of hydrogel was kept at 100 °C for 3 min to turn off the enzyme. Next, 50 μL of a potassium tetraborate solution (4.94 g of boric acid and 1.98 g of potassium hydroxide dissolved in 100 mL ultrapure water, half-life at 4 °C of 15 days) were added to the solution which was homogenized through stirring and then returned to 100 °C for 3 min to create the complex between potassium tetraborate and *N*-acetylglucosamine ends groups that reacts with DMAB to create the colored complex. After that, 1.5 mL of a dilute solution (1/10) of DMAB obtained by diluting the stock solution (5 g of DMAB dissolved in 6.25 mL of 12 M HCl and made up to 50 mL with glacial acetic acid, can be stored for 1 month at 4 °C) were added to the samples which were kept at 37 °C during 15 min, and then analyzed in a UV-visible spectrophotometer (Cary 100 bio, Varian, USA) in a range of 400 at 700 nm.

3. Results and discussions

3.1 Synthesis of HA-*g*-P(iPrOx-*co*-BuOx)

HA-*g*-P(iPrOx-*co*-BuOx) was prepared from the CROP (cationic ring-opening polymerization) reaction between 2-*n*-isopropyl-2-oxazoline (iPrOx), 2-*n*-butyl-2-oxazoline (BuOx), and tetrabutylammonium hyaluronate as shown on the reaction mechanism in Fig. 1.[34,35] The ^{1}H NMR characterization for HA-*g*-P(iPrOx-*co*-BuOx) and P(iPrOx-*co*-BuOx) is shown in the ESI† (S1 and S2). The DS, DP, and the IPrOx/BuOx ratio are determined as explained in our previous work.[34] The substitution degree (DS) was determined according to eqn (2) (more information in the ESI†).

$$\text{DS} = \frac{3 \times I_{3.5\text{ppm-}10}}{4 \times \text{DP} \times I_{1.88\text{ppm}}} \quad (2)$$

Ideal conditions for hydrogel injection/gelation were achieved at an experimental iPrOx/BuOx ratio of 67/33 (±1/1), a DS of 10 (±3), and a DP of 25 (±5).

Rheological measurement of this sample has been done to check its gelation ability when heated to 37 °C (body

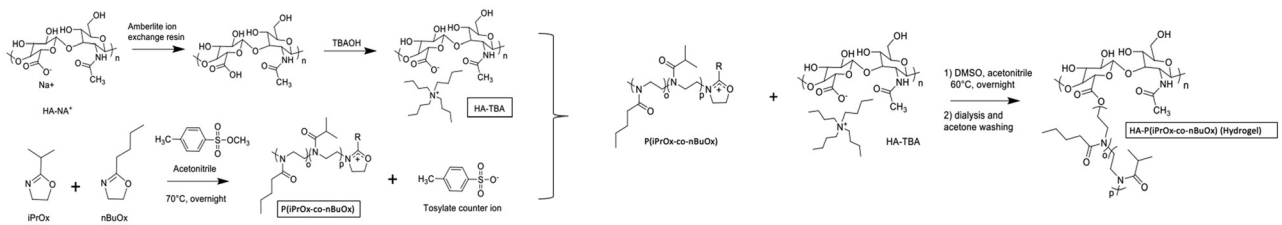

Fig. 1 Reaction mechanism for grafting the P(iPrOX-*co*-BuOx) copolymer onto hyaluronic acid.

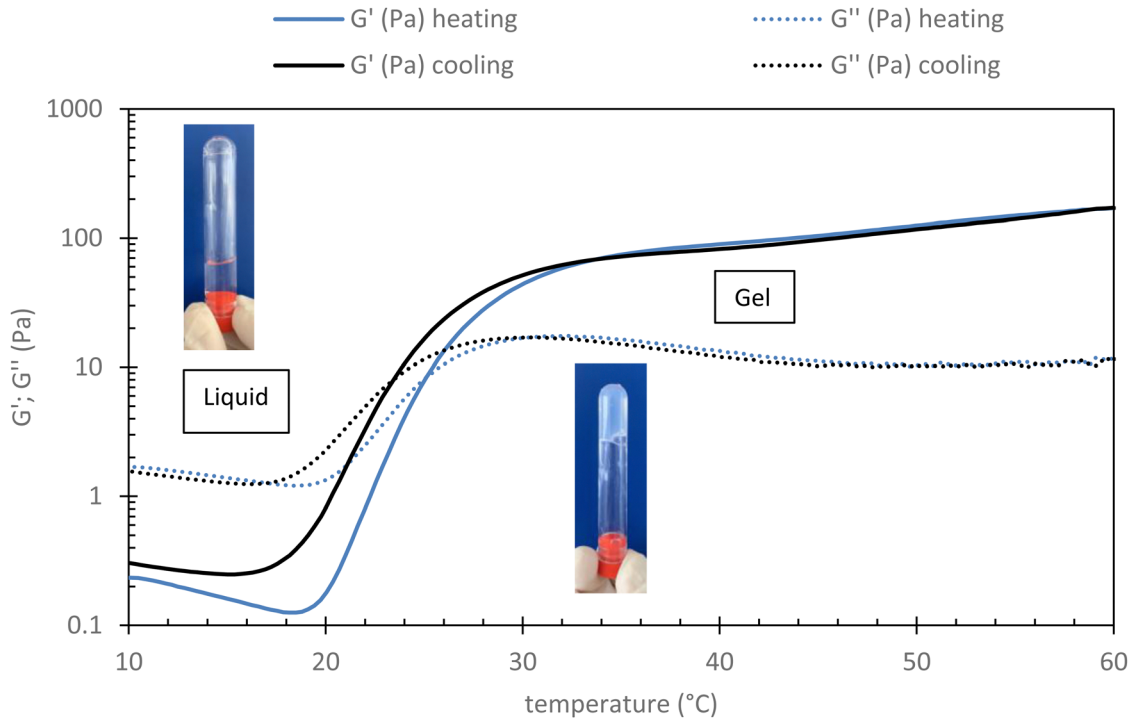

Fig. 2 Evolution of rheological profile of HA-*g*-P(iPrOx-*co*-BuOx-67/33)-0.10 015 g L^{-1} in NaCl 0.15 M in function of temperature (shear stress: 0.1 Pa; frequency: 1 Hz and rate: 0.5 °C min^{-1}).

temperature). As shown in Fig. 2 (see part 2.3.2 for conditions), it can be observed that below 20 °C, G'' is largely above G' indicating the viscous state of the system, which is therefore expected to be easily injectable. In this range both moduli decrease with the temperature according to thermal agitation, this behavior is typical of water-soluble polymer dynamic. After 20 °C, both moduli increase with the temperature as the grafted POX chains start to associate themselves (explained by their LCST character). The associative behavior is reinforced with the increase of the temperature. Thus, and logically, G' increases more than G'' leading to a critical temperature, sometimes called transition temperature ($T_{sol/gel}$), that corresponds to the crossover of both moduli. Finally, the elastic modulus seems to reach a plateau (~100 Pa) from about 35 °C. It is largely higher than the G'' (more than 1 decade), which means that the elastic behavior of the material is predominant over its viscous behavior.

This result seems to indicate that this sample is well adapted for human body medical sol/gel application in terms of the temperature of final gelation (~37 °C) and of the magnitude of the elastic modulus.

3.2 Hydrogel stability at 37 °C

To ensure that the hydrogel remains in the gel state at 37 °C, a 24-hour rheological analysis was set up in oscillatory mode (measurement of G' and G'' moduli for 24 h at 37 °C, 0.1 Pa, and 1 Hz).

As shown in Fig. 3, it can be seen that the elastic modulus G' remains higher than the viscous modulus G'' for at least 15 h at 37 °C, above this time, solvent evaporation probably occurs leading to an increase in both moduli. This confirms that the hydrogel remains stable at 37 °C for at least 15 h (maximum operating conditions). One can notice a very slight diminishing of both moduli over time that could be explained by a possible reorganization in the associations, without changing the main behavior.

A second study on the same sample (*i.e.* HA-*g*-P(iPrOx-*co*-BuOx-67/33)-0.10) was designed to confirm whether the hydrogel remained stable in an excess of solvent at 37 °C. The hydrogel was immersed in an excess of a 0.15 M NaCl solution. Then, supernatant samples were taken off every day to check if some polymer was extracted from the gel toward the supernatant. These samples were analyzed by TOC to follow the variation in carbon content in the supernatant as a function of time for 5 days, and thus to trace the release polymer concentration in the supernatant, as shown in Fig. 4(A).

Regarding this sample, it appears that only 0.9 g L^{-1} has been released after 5 days which represents less than 6% of the initial amount of polymer in the gel. This result clearly indicates that the gel is strongly stable in an excess of solvent at the body temperature. The burst effect observed during the first 6 hours can be explained by the diffusion of polymers which should not be correctly crosslinked with a major part of hydrogel in the supernatant.

To confirm these results, a third study was carried out to control the swelling rate of the hydrogel over time in order to prove that the hydrogel remains in the gel state for at least 5 days even with the presence of a solvent excess applied to its

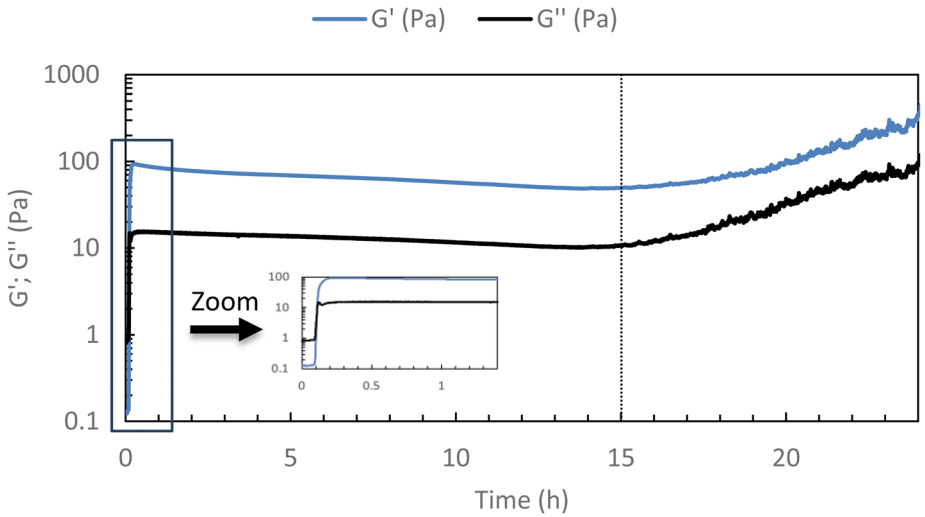

Fig. 3 Stability studies of HA-*g*-P(iPrOx-*co*-BuOx-67/33)-0.10 at 37 °C (15 g L^{-1} in NaCl 0.15 M) for 24 h (0.1 Pa and 1 Hz).

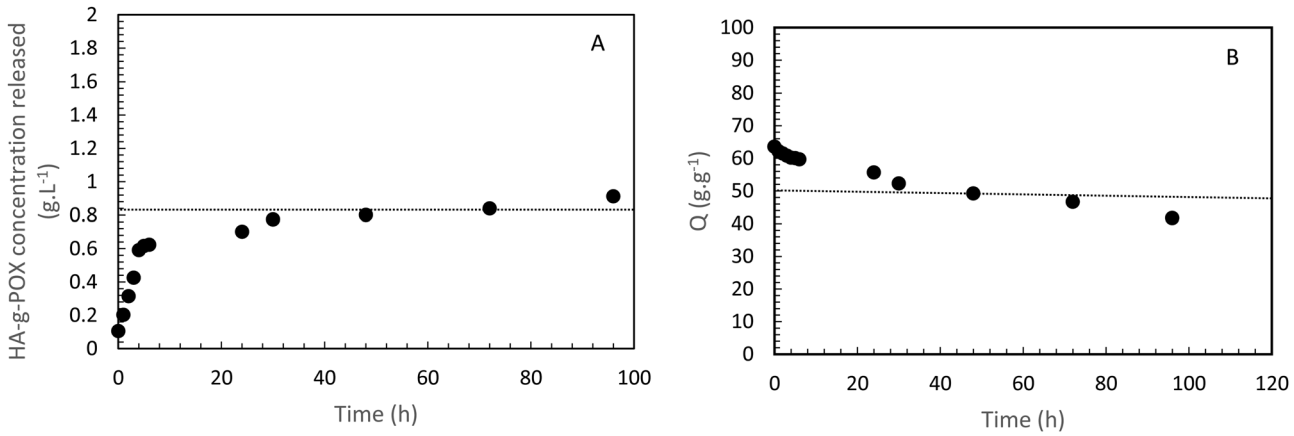

Fig. 4 HA-*g*-P(iPrOx-*co*-BuOx-67/33)-0.10 concentration released in the supernatant over time at 37 °C. B-Swelling rate (*Q*) of HA-POX over time at 37 °C.

surface. As can be seen in Fig. 4(B), 80% of the initial swelling is conserved after 5 days. The swelling loss observed seems to be correlated to the loss of polymer (6%) observed during the TOC analysis described above. Finally, over the experimental time of 15 hours induced by rheological limits, our swelling and polymer release results confirm that the gel state is globally preserved over 5 days.

3.3 Enzymatic degradation

The enzymatic degradation preliminary study of the hydrogel in the presence of hyaluronidase (Fig. 5(A)) shows that the reducing ends groups (*N*-acetylglucosamine or NAG) concentration is higher when the HA-*g*-POX degradation is done at 20 °C than at 37 °C after 72 h (1.3 mmol L^{-1} at 20 °C *vs.* 0.3 mmol L^{-1} at 37 °C). More importantly, the HA-*g*-POX degradation at 37 °C reaches a plateau after one hour, whereas HA-*g*-POX degradation at 20 °C increases over time. This plateau may be explained by the fact that, at 37 °C, the hydrogel's polyoxazoline grafts limit access to the glycosidic β (1–4) bond of hyaluronic acid, in addition to the gel structure, which greatly slows down the enzyme.

To better visualize the phenomenon, the evolution of the number average molar mass (M_n, determined using eqn (3)) was plotted as a function of time for the hydrolysis undergone by the gel.

$$M_n = \frac{[\text{Hydrogel}]_m}{[\text{E.R}]_{\text{mol L}^{-1}}} \quad (3)$$

As shown in Fig. 5(B), for the solution at 20 °C, the molar masses decrease to reach an M_n of around 10 000 g mol^{-1} after 5 days, unlike the gel at 37 °C, which degrades to around 52 000 g mol^{-1}. If we compare this result with the literature,[39] the total degradation of native hyaluronic acid leads to a M_n of about 1600 g mol^{-1}, that means about 4 disaccharide units.

Thus, our results show that HAase leads to a degradation of HA-*g*-POx which is largely less important as compared to native HA. This is due to the presence of the grafted POx groups which limit the accessibility of the enzyme. Moreover, at the gel state,

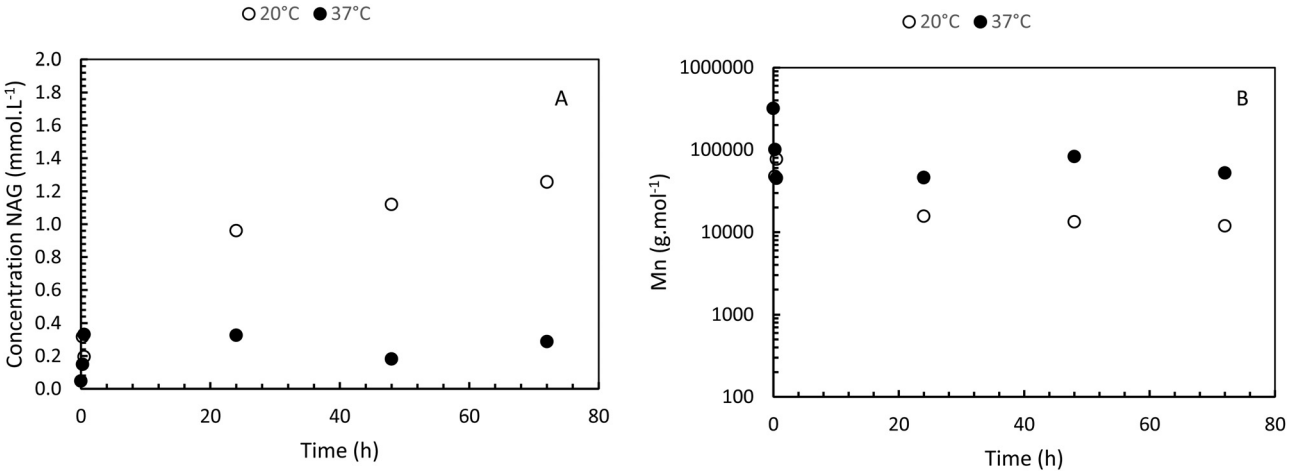

Fig. 5 (A) Enzymatic degradation of HA-*g*-P(iPrOx-*co*-BuOx-67/33)-0.10 in presence of hyaluronidase (100 μL at 1 mg mL^{-1} for 10 mL hydrogel at 15 g L^{-1}) over time at 20 °C and 37 °C. (B) Molar mass evolution of HA-*g*-P(iPrOx-*co*-BuOx-67/33)-0.10 over time in presence of hyaluronidase at 20 °C and 37 °C.

the degradation is more limited than at the sol state due probably to the hindering of the network. As reported in part 3.2 this slight enzymatic degradation at the gel state does not lead to the destructuration of the network. These results are very encouraging for future applications.

3.4 Hydrogel injectability

3.4.1 Hydrogel injectability at 20 °C. To ensure the feasibility of an *in vivo* injection, it was essential to check that the injection did not cause any irreversible damage to the hyaluronic acid chains, thus preventing gelation. To this end, a rheological protocol was set up. In the first step, the flow behavior of the modified HA-*g*-P(iPrOx-*co*-BuOx-67/33)-0.10 solution at 15 g L^{-1} in 0.9% NaCl was followed at 20 °C (Fig. 6). It can be observed that the hydrogel presents a mainly Newtonian behavior followed by a starting shear thinning one from 50 s^{-1} approximately. One can also notice the non-thixotropic behavior. This flow can be correctly modelized thanks to the Williamson empirical relation (eqn (4)):

$$\eta_{(\dot{\gamma})} = \frac{\eta_0}{1 + (K\dot{\gamma})^n} \quad (4)$$

where η_0 is the Newtonian viscosity, K is the consistency (time of disentanglement), and n is the shear thinning index.

The Williamson model well fits the experimental flow curve of the solution (R^2 = 0.9996) and gives the following result: η_0 = 155 mPa s^{-1}; K = 5 ms; n = −0.77. This behavior is a good indication and prognostic of potential easy injectability.

In the following, G' and G'' (at 1 Hz) are measured under various conditions of stress and temperature. Step 0 gives the original elastic state of the hydrogel at 37 °C in the linearity domain (low stress: 0.1 Pa, 1 Hz). Then, the hydrogel was

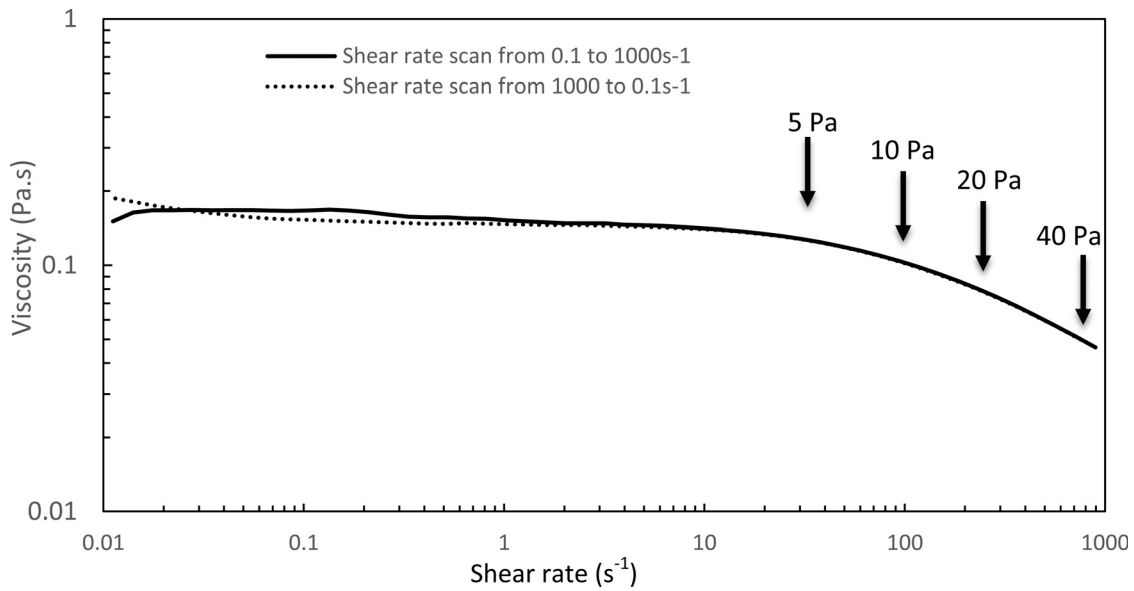

Fig. 6 Flow curve for HA-*g*-P(iPrOx-*co*-BuOx-67/33)-0.10 at 20 °C; 15 g L^{-1}.

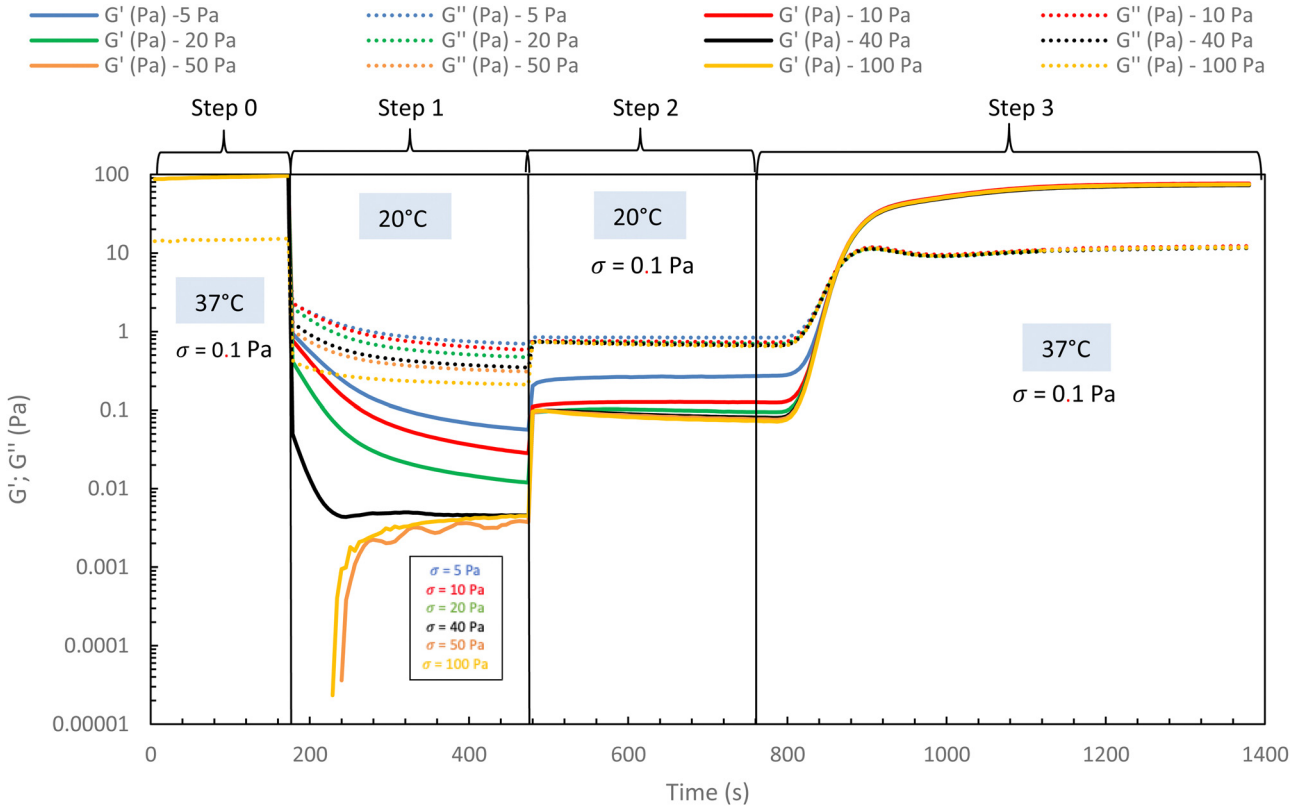

Fig. 7 Rheological injection simulation for HA-*g*-(PiPrOx-*co*-PBuOx-67/33)-0.10 *via* different stress apply at 20 °C to mimic the injection phenomenon (15 g L^{-1} in NaCl 0.15 M).

subjected to various stresses at 20 °C ranging from 5 to 100 Pa during 5 min (step 1 in Fig. 7). Thus, this step simulates the applied stress when the hydrogel is injected *via* a syringe with a needle or capillary. These stresses were reported with their corresponding viscosities in Fig. 6 (flow curve), which evidences that the tested stresses correspond to the shear thinning behavior range. The hydrogel is then left to rest at 20 °C under very low stress (0.1 Pa) for 5 minutes (step 2 in Fig. 7). This stage mimics the moment when the gel exits the syringe/needle and enters the human body (with no stress applied and not heated at 37 °C yet). Finally, during step 3 (Fig. 7), the geometry is heated to 37 °C to mimic the introduction in the human body in the same conditions as step 0. In a second stage (Fig. 8), the same analysis was carried out, but instead of applying stress to the hydrogel *via* the rheometer, it was injected into the device geometry using different syringes, needles, micropipettes, and capillaries (*cf.* S3 ESI† for capillaries experiments).

As shown in Fig. 7 and 8, whatever the applied stress and whatever the used injection method, the hydrogel will regain its initial properties at 37 °C very quickly. The time frame between the temperature set and the beginning of the modulus increase is about 150 s. It can be easily explained and has to be subtracted to the time of gelation. Indeed, the time needed by the Peltier temperature control to reach the set temperature inside the geometry (double wall concentric cylinder) was found to be 290 s. This time becomes largely lower if another geometry with less metal envelope, such as a cone-plate geometry, is used. Otherwise, these results also indicate that injections do not cause irreversible damage to the polymer and do not affect the thermo-gelling behavior. Thus, we confirm that such thermosensitive hydrogels are perfectly injectable, whatever the injection used method.

3.4.2. Hydrogel injectability at 37 °C. Although the injection does not take place at 37 °C, we wanted nevertheless to study the behavior of the system if injected at 37 °C, *i.e.*, in the gelled state. To this end, a rheology protocol was set up to apply various stresses to the hydrogel at 37 °C. Between each stress application, it was ensured that the system returned to its initial state (step 0 in Fig. 8: 0.1 Pa, 1 Hz, 30 minutes in contrast to the stress application, which only lasted for 5 minutes).

Excepted for both 50 and 100 Pa which are not strong enough to completely break the structure of the hydrogel at 37 °C, the results of Fig. 9 show that the high shear stresses lead to a decrease in moduli due to the disorganization of the physically associated network. This becomes noticeable from 150 Pa with G' lower than G'' (that means a liquid and viscous state). Whatever the applied stress, once the stress is removed, the hydrogel returns very quickly to its initial gelled state without irreversible damage.

3.5 Incorporation of a secondary network (semi-interpenetrating network (IPN))

For future applications, we could be led to add new properties to the hydrogel, such as contrast agents, drug delivery molecules, and others. Thus, it appears to be easier to modify a new

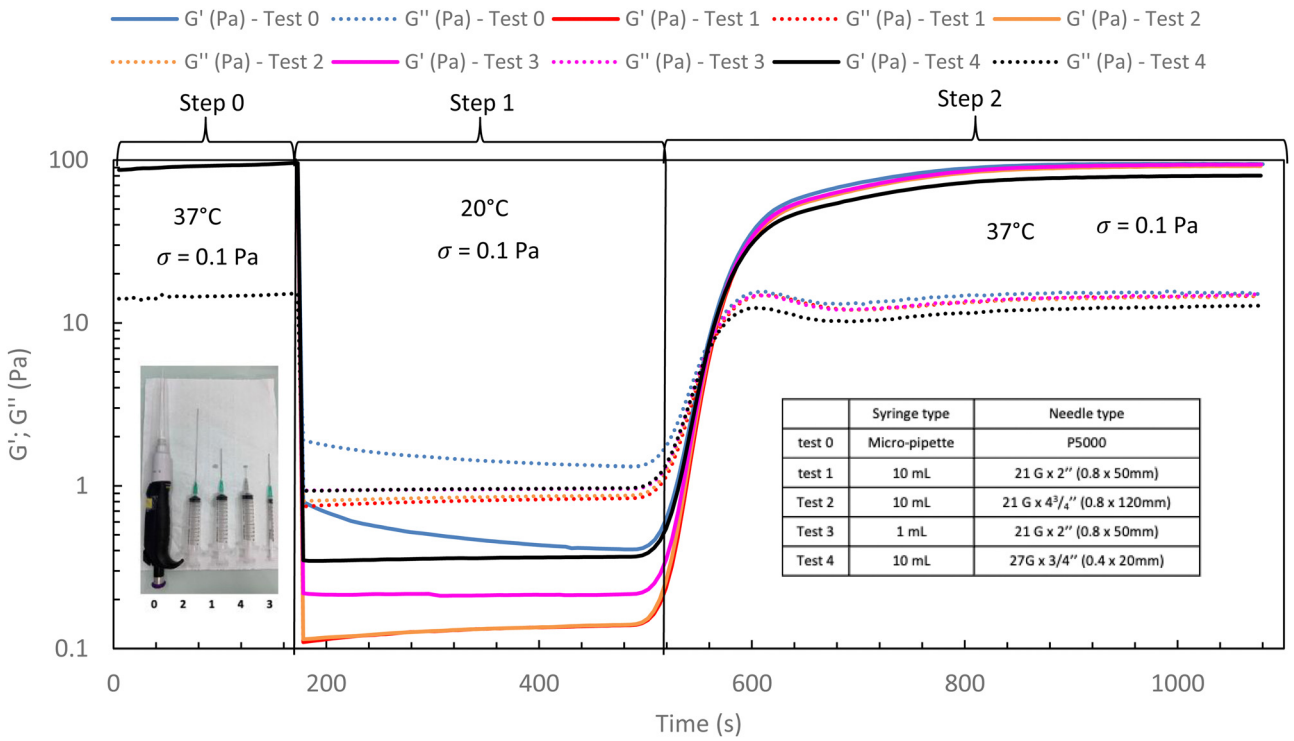

Fig. 8 Rheological *in situ* injection *via* different syringes and needles for HA-PiPrOx-*co*-PBuOx-66/34-0.10 at 20 °C to mimic the injection phenomenon (15 g L^{-1} in NaCl 0.15 M).

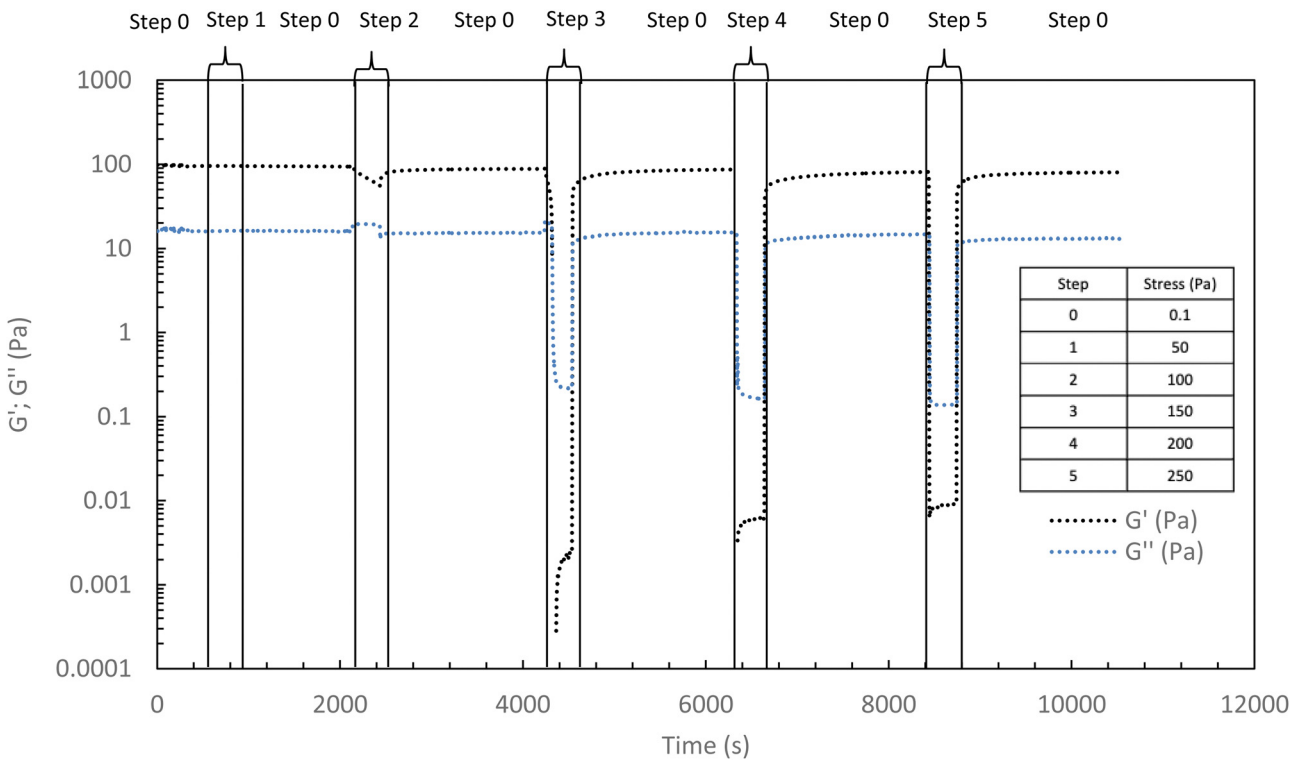

Fig. 9 Elastic and viscous moduli during different stresses applications (ranging from 50 to 250 Pa) to the hydrogel (HA-PiPrOx-*co*-PBuOx-66/34-0.10, 15 g L^{-1} in NaCl 0.15 M) at 37 °C (1 Hz) with a rest time (0.1 Pa, 1 Hz) between stresses.

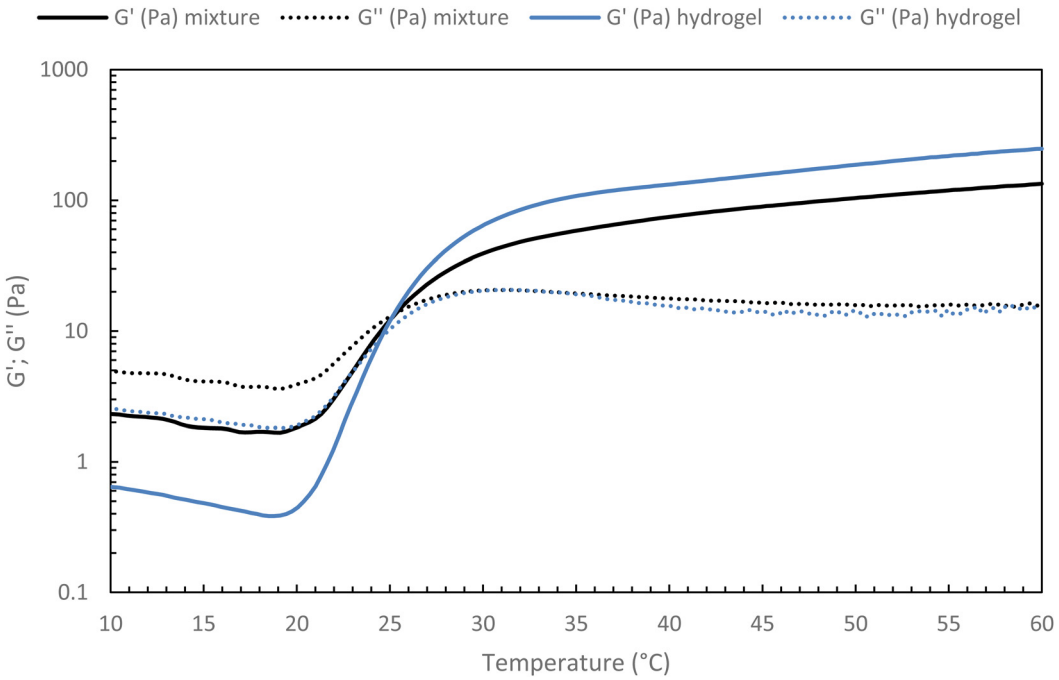

Fig. 10 Temperature ramp for hydrogel alone (HA-*g*-(PiPrOx-*co*-PBuOx-67/33)-0.10) and hydrogel/HA mixture (75/25 – v/v) at 15 g L^{-1} in NaCl 0.15 M (0.1 Pa and 1 Hz; 0.5 °C min^{-1}).

native HA than an already thermo-sensitive HA. Indeed, the chosen strategy for a potential medical application will be to graft the various molecules onto new native HA chains and blend them into the thermosensitive hydrogel network. It must then be ensured that the incorporation of a secondary network based on native HA does not prevent the thermosensitive hydrogel from gelling.

To confirm this strategy, a 15 g L^{-1} solution of the heat-sensitive HA-*g*-P(iPrOx-*co*-BuOx-67/33)-0.10 was mixed with 15 g L^{-1} native HA solution at different volume ratios at 4 °C and the gelation of the resulting mixture were then monitored. To begin, a mixture with a volume ratio of 75/25 thermosensitive/native HA was studied (Fig. 10). One can notice a slight

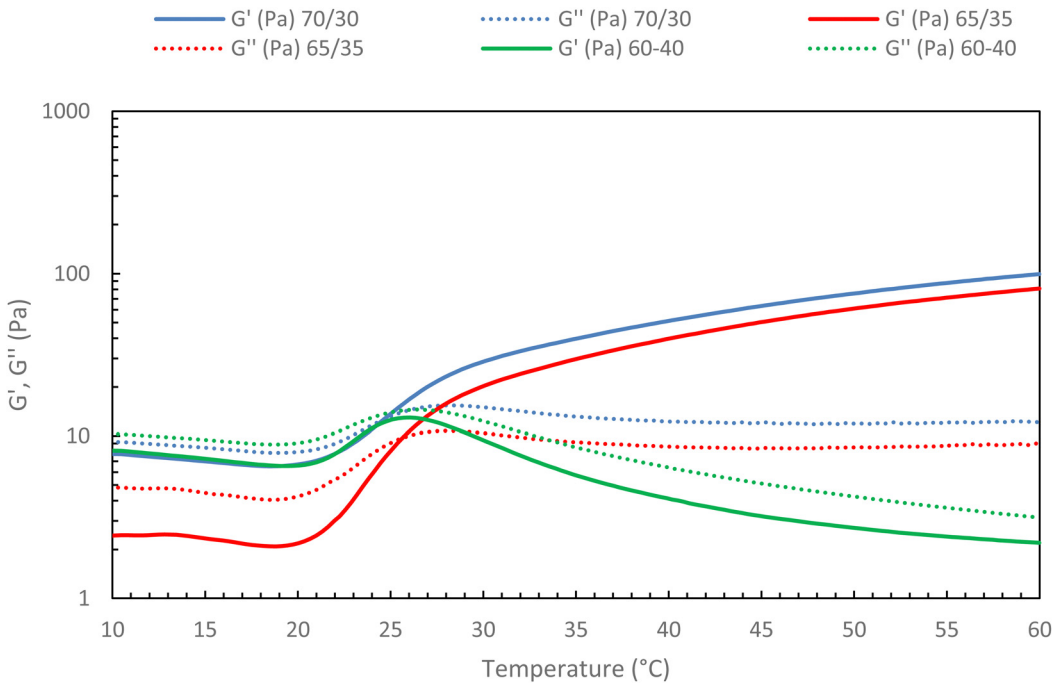

Fig. 11 Rheological ramp of different mixture between HA-*g*-P(iPrOx-*co*-BuOx-67/33)-0.10 and native HA (15 g L^{-1} in NaCl 0.15 M; 0.5 °C min^{-1}, 0.1 Pa and 1 Hz).

decrease in G' modulus for the hydrogel/HA mixture compared with the hydrogel alone. This drop in modulus can be explained by the secondary hyaluronic acid network which will prevent certain physical cross-linking nodes from forming that leads to a weakened 3D network. Nevertheless, the respective gelation temperature of the mixture and the corresponding thermosensitive HA remain identical, which is a promising feature for future research.

Then, the native HA content in the mixture ratio was increased to find out whether a limit should not be exceeded to preserve the gelation of the mixture. To this end, different HA-*g*-P(iPrOx-*co*-BuOx-67/33)-0.10/native HA ratios were tested, and the results are presented in Fig. 11.

The first thing to note is that the more secondary network is added to the mixture, the more G' decreases. This confirms that the secondary network will prevent certain cross-linking nodes from forming as was hypothesized above. Indeed, the more secondary network is added, the more difficult it becomes for the polyoxazoline chains to associate with each other to form the gel, up until a critical point is reached where gelation becomes impossible. Indeed, the absence of a crossover point between G' and G'' moduli is evidenced for a 60/40 ratio (green curves) in Fig. 11, with G'' being higher than G' throughout the temperature range. This behavior indicates the absence of gelation in the system, implying that it will be impossible to add a secondary network in proportions greater than 35% without losing the thermosensitive character of the mixture at 15 g L^{-1}. This is an encouraging result, as it indicates that the incorporation of hyaluronic acid modified with molecules of interest should be feasible for future studies.

Studies of stability (S6 supporting data, ESI†), flow behavior (S7 supporting data, ESI†), and injectability (S8 supporting data, ESI†) of the 75/25 ratio mixtures are perfectly similar in terms of interpretation to the pure thermosensitive systems discussed above.

Conclusions

Following on from our previous work,[34] the thermoresponsive HA-*g*-P(iPrOx-*co*-BuOx) copolymer was designed to be ideally suited to an injectable biomedical application. We obtained a grafting of the P(iPrOx-*co*-BuOx) copolymer (67/33 molar ratio; DP: 25) with a grafting rate of around 10%. This grafting results in a reversible thermosensitive hydrogel (at 15 g L^{-1}) with a G', G'' crossover point of around 25 °C (for a G' at 37 °C of around 80 Pa ± 20). We have shown that this hydrogel is perfectly stable at 37 °C for at least 5 days. We have also demonstrated that the gel is maintained when submitted to HAase action for 4 days, even if some chain cuts occur. These are very encouraging results for future applications in the human body, but further studies will be necessary notably *in vivo* for which other variables could occur. In addition, the slight shear thinning behavior of the solution at 20 °C led to comfortable injectability conditions. Nevertheless, in the gel state, injectability measurements showed high resistance, requiring the hydrogel to be subjected to high stresses leading to the breaking of the 3D network. However, once the stress is removed, the gel network reforms very quickly without causing irreversible damage to the polysaccharide chains. These good results prompted us to try the incorporation of a secondary network (HA) inside the heat-sensitive hydrogel, with the aim of grafting therapeutic molecules onto it at a later stage. The results obtained showed that a secondary network could be added to the hydrogel in a maximum proportion of 35 wt%. The mixed gel showed a slight loss of G' modulus at 37 °C but remained stable at 37 °C for at least 3 days and had the same injection ability as the hydrogel alone. These results are very encouraging and allow us to envisage the incorporation of therapeutic molecules in the future.

Author contributions

Morgane Morel: investigation, writing the original draft. Mathieu Madau: supervision – writing – review & editing. Virginie Dulong: supervision – writing – review & editing. Anne-Claire Groo: supervision – writing – review & editing. Aurélie Mazert-Fréon: supervision – writing – review & editing. Didier Le Cerf: supervision – writing – review & editing. Luc Picton: supervision – writing – review & editing.

Conflicts of interest

The authors declare that they have no known competing financial interests or personal relationships that could have appeared to influence the work reported in this paper.

Acknowledgements

The authors would like to thank the Normandy region for their financial contribution to the RIN TREMPLIN NeuroOncoChimie project (ERDF funding). The authors would also like to thank Koceila Boundaoui for his help with injectability studies at 37 °C.

References

1 C. Zhao, L. Zhou, M. Chiao and W. Yang, *Adv. Colloid Interface Sci.*, 2020, **285**, 102280.
2 I. Tokarev and S. Minko, *Soft Matter*, 2009, **5**, 511–524.
3 M. Hamidi, A. Azadi and P. Rafiei, *Adv. Drug Delivery Rev.*, 2008, **60**, 1638–1649.
4 S. Mantha, S. Pillai, P. Khayambashi, A. Upadhyay, Y. Zhang, O. Tao, H. M. Pham and S. D. Tran, *Materials*, 2019, **12**(20), 3326.
5 M. C. Catoira, L. Fusaro, D. Di Francesco, M. Ramella and F. Boccafoschi, *J. Mater. Sci.: Mater. Med.*, 2019, **30**, 115.
6 M. Guenther, G. Gerlach, T. Wallmersperger, M. N. Avula, S. H. Cho, X. Xie, B. V. Devener, F. Solzbacher, P. Tathireddy, J. J. Magda, C. Scholz, R. Obeid and T. Armstrong, *Adv. Sci. Technol.*, 2013, **85**, 47–52.

7 A. C. Jen, M. C. Wake and A. G. Mikos, *Biotechnol. Bioeng.*, 1996, **50**, 357–364.
8 T. R. Hoare and D. S. Kohane, *Polymer*, 2008, **49**, 1993–2007.
9 J. Lou and D. J. Mooney, *Nat. Rev. Chem.*, 2022, **6**, 726–744.
10 S. Graham, P. F. Marina and A. Blencowe, *Carbohydr. Polym.*, 2019, **207**, 143–159.
11 L. Yu and J. Ding, *Chem. Soc. Rev.*, 2008, **37**, 1473–1481.
12 D. J. Overstreet, D. Dutta, S. E. Stabenfeldt and B. L. Vernon, *J. Polym. Sci., Part B: Polym. Phys.*, 2012, **50**, 881–903.
13 E. Hasanzadeh, A. Seifalian, A. Mellati, J. Saremi, S. Asadpour, S. E. Enderami, H. Nekounam and N. Mahmoodi, *Mater. Today Bio*, 2023, **20**, 100614.
14 C. Mo, R. Luo and Y. Chen, *Macromol. Rapid Commun.*, 2022, **43**, 2200007.
15 M. Norouzi, J. Firouzi, N. Sodeifi, M. Ebrahimi and D. W. Miller, *Int. J. Pharm.*, 2021, **598**, 120316.
16 J. Basso, A. Miranda, S. Nunes, T. Cova, J. Sousa, C. Vitorino and A. Pais, *Gels*, 2018, **4**, 62.
17 J. Zhang, C. Chen, A. Li, W. Jing, P. Sun, X. Huang, Y. Liu, S. Zhang, W. Du, R. Zhang, Y. Liu, A. Gong, J. Wu and X. Jiang, *Nat. Nanotechnol.*, 2021, **16**, 538–548.
18 M. D'Este, M. Alini and D. Eglin, *Carbohydr. Polym.*, 2012, **90**, 1378–1385.
19 G. Mocanu, D. Mihaï, V. Dulong, L. Picton and D. Le Cerf, *Carbohydr. Polym.*, 2012, **87**, 1440–1446.
20 R. Hoogenboom and H. Schlaad, *Polym. Chem.*, 2016, **8**, 24–40.
21 D. J. Overstreet, R. Y. McLemore, B. D. Doan, A. Farag and B. L. Vernon, *Soft Mater.*, 2013, **11**, 294–304.
22 V. Dulong, G. Mocanu, L. Picton and D. Le Cerf, *Carbohydr. Polym.*, 2012, **87**, 1522–1531.
23 P. M. Niang, Z. Huang, V. Dulong, Z. Souguir, D. Le Cerf and L. Picton, *Carbohydr. Polym.*, 2016, **139**, 67–74.
24 G. Mocanu, Z. Souguir, L. Picton and D. Le Cerf, *Carbohydr. Polym.*, 2012, **89**, 578–585.
25 X. Xu, Y. Liu, W. Fu, M. Yao, Z. Ding, J. Xuan, D. Li, S. Wang, Y. Xia and M. Cao, *Polymers*, 2020, **12**, 580.
26 T. X. Viegas, M. D. Bentley, J. M. Harris, Z. Fang, K. Yoon, B. Dizman, R. Weimer, A. Mero, G. Pasut and F. M. Veronese, *Bioconjugate Chem.*, 2011, **22**, 976–986.
27 A. L. Fisher, J. M. H. Schollick, D. G. A. L. Aarts and M. C. Grossel, *RSC Adv.*, 2016, **6**, 66438–66443.
28 A. Bogomolova, S. K. Filippov, L. Starovoytova, B. Angelov, P. Konarev, O. Sedlacek, M. Hruby and P. Stepanek, *J. Phys. Chem. B*, 2014, **118**, 4940–4950.
29 A. Amirova, S. Rodchenko, M. Kurlykin, A. Tenkovtsev, I. Krasnou, A. Krumme and A. Filippov, *Polymers*, 2020, **12**, 698.
30 A. Borzacchiello, L. Russo, B. M. Malle, K. Schwach-Abdellaoui and L. Ambrosio, *BioMed Res. Int.*, 2015, **2015**, e871218.
31 J. A. Burdick and G. D. Prestwich, *Adv. Mater.*, 2011, **23**, H41–H56.
32 S. Federico, U. Nöchel, C. Löwenberg, A. Lendlein and A. T. Neffe, *Acta Biomater.*, 2016, **38**, 1–10.
33 I. S. Bayer, *Molecules*, 2020, **25**, 2649.
34 M. Madau, G. Morandi, V. Lapinte, D. Le Cerf, V. Dulong and L. Picton, *Polymer*, 2022, **244**, 124643.
35 M. Madau, G. Morandi, C. Rihouey, V. Lapinte, H. Oulyadi, D. L. E. Cerf, V. Dulong and L. Picton, *Polymer*, 2021, **230**, 124059.
36 G. Alonci, R. Mocchi, S. Sommatis, M. C. Capillo, E. Liga, A. Janowska, L. Nachbaur and N. Zerbinati, *Pharmaceutics*, 2021, **13**, 1194.
37 Y. Li, X. Zhang, X. Liu, W. Pan, N. Li and B. Tang, *Chem. Sci.*, 2021, **12**, 3130–3145.
38 J. L. Reissig, J. L. Strominger and L. F. Leloir, *J. Biol. Chem.*, 1955, **217**, 959–966.
39 H. Duan, M. Donovan, F. Hernandez, C. Di Primo, E. Garanger, X. Schultze and S. Lecommandoux, *Angew. Chem., Int. Ed.*, 2020, **59**, 13591–13596.